Incompletely Stirred Reactor Network modeling for the estimation of turbulent non-premixed autoignition

Salvatore Iavarone, Savvas Gkantonas, Epaminondas Mastorakos
University of Cambridge
Cambridge, United Kingdom

1 Introduction

Autoignition in turbulent reactive flows is a lingering problem of fundamental importance and practical interest. The understanding of the complex interactions between turbulence, micro-mixing and chemistry, leading to autoignition, is crucial to the design of several combustion devices. In such applications, autoignition occurs in the presence of considerable fluctuations of temperature, velocity, and composition, whose effect must be understood and predicted. Particularly, the minimization of the autoignition risk is critical to the design of premixers of aeroderivative gas turbines, especially when highly reactive fuels such as hydrogen or higher hydrocarbons are used. For these purposes, Markides and Mastorakos [2] performed experiments of autoignition of a hydrogen plume, diluted with nitrogen, issued into a co-flow of preheated air at atmospheric pressures. In the experimental campaign, different auto-ignition regimes, i.e., "no ignition", "random spots", flashback and lifted flame, were observed depending on the co-flow temperature and the ratio between co-flow and fuel velocities. It was shown that the observed auto-ignition length decreased with an increase of the co-flow temperature and a decrease of the velocity ratio. Several numerical studies tried to replicate the regimes observed by Markides and Mastorakos with the Conditional Moment Closure model [3] coupled with either RANS [5–7], or LES approaches [8]. The transported PDF model was also employed with LES in [4]. In all these studies, the focus was on auto-ignition in the case of equal fuel and air velocities. None of the above-mentioned studies considered non-adiabatic conditions, i.e, radiative and convective heat transfer from the flow to the surrounding quartz tube, and the effect of differential diffusion. The objectives of the present work are twofold. First, we introduce an Incompletely Stirred Reactor Network (ISRN) formulation for capturing autoignition in turbulent flows. Namely, ISRN solves the conditional average species and enthalpy transport equations in a post-processing fashion, with the conditioning performed on the mixture fraction, and on top of an inert flow solution provided by LES, similar to what was attempted previously for emissions modelling [10, 11]. Second, we investigate the effects of non-adiabatic conditions and differential diffusion on the prediction of hydrogen autoignition.

2 Methodology

In the experiments performed by Markides et al. [2], hydrogen diluted with nitrogen ($Y_{\mathrm{H_2}}$=0.13 and $Y_{\mathrm{N_2}}$=0.87) was injected in a turbulent co-flow of heated air and grid-generated turbulence. The stoichiometric mixture fraction, ξ_{ST}, is 0.184. The fuel was injected into the co-flow through a 2.24 mm

Correspondence to: si339@cam.ac.uk

diameter (d) nozzle at ambient pressure (see Fig. 1). The burner inner diameter is 24.8 mm. Co-flow air velocities (U_{ox}) up to 35 m/s, with temperatures (T_{ox}) up to 1015 K, were achieved. The fuel velocity (U_f) ranged from 20 to 120 m/s, with temperatures between 650 K and 930 K. Air was electrically preheated and flowed into a circular quartz tube, after passing through a perforated plate to promote turbulence. Different auto-ignition regimes (no ignition, random spots, flashback and lifted flame) were obtained by varying the air temperature and inlet velocity. Regions of presence of OH chemiluminescence were considered as "auto-ignition spots" [2].

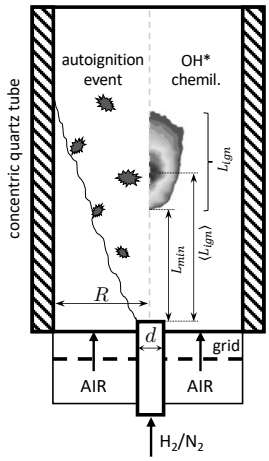

Figure 1: Apparatus schematic (not to scale) with indication of autoignition events (left) and representative averaged OH* chemiluminescence contour (right) [2].

2.1 Non-reactive flow simulation

In this work, the Large Eddy Simulation (LES) of the burner is carried out using the software CONVERGE. The sub-grid scales are modelled using the Dynamic Smagorinsky model based on the eddy viscosity approach. PISO scheme and an implicit first-order temporal scheme are employed for solving the governing equations of the flow. The experimental velocity profiles are imposed at both fuel and air inlets along with Dirichlet boundary conditions for species mass fractions and pressure. At the outlet, zero gradient (Neumann) boundary conditions are enforced for velocity components and species mass fractions and the pressure is fixed to the atmospheric value. Walls are defined as no-slip with zero velocity and species concentration without wall functions. They are also assumed adiabatic. A digital filter is used for synthetic turbulence with intensity I = 0.15 and length scale L_{turb} = 0.004 m. The turbulent Schmidt number Sc_t is set to 0.4. Adaptive Mesh Refinement with minimum cell size δ = 0.125 mm is employed, resulting in a total number of cells ≈2.5M. User Defined Functions (UDF) are set up for the estimation of the subgrid mixture fraction variance and the scalar dissipation rate, which are input quantities for the subsequent ISRN approach.

2.2 ISRN approach

In CMC, transport equations are solved for the conditionally averaged reacting scalars Q, which are conditioned on the mixture fraction ξ. When CMC is used, it is common practice to use a dual mesh approach, where the CMC grid is coarser than the LES one. Assuming steady-state and neglecting turbulent transport in the longitudinal direction by conditional fluctuations, i.e., thin-shear flow, the CMC shear flow equations can be obtained from the canonical form of the CMC equations by averaging

across the flow [3]. The present formulation accounts for the effect of differential diffusion, i.e., non-unity Lewis numbers, and thus the governing equations for the i-th conditionally averaged species mass fraction, Q_i, and the conditionally averaged enthalpy, Q_h, can be written as

$$U^* \frac{\partial Q_i}{\partial z} = \frac{\partial}{\partial z}\left(D_t^* \frac{\partial Q_i}{\partial z}\right) + \langle \dot{\omega}_i | \eta \rangle + \frac{N^*}{Le_i}\frac{\partial^2 Q_i}{\partial \eta^2} + \left(\frac{1}{Le_i} - 1\right) M^* \frac{\partial Q_i}{\partial \eta}, \tag{1}$$

$$\begin{aligned} U^* \frac{\partial Q_h}{\partial z} =& \frac{\partial}{\partial z}\left(D_t^* \frac{\partial Q_h}{\partial z}\right) + \langle \dot{\zeta}_i | \eta \rangle + N^* \frac{\partial^2 Q_h}{\partial \eta^2} + N^* \frac{\partial Q_h}{\partial \eta} \sum_{i=1}^{N} \left(\frac{1}{Le_i} - 1\right) \frac{\partial Q_i}{\partial \eta} \\ &+ N^* Q_h \sum_{i=1}^{N} \left(\frac{1}{Le_i} - 1\right) \frac{\partial^2 Q_i}{\partial \eta^2} + M^* Q_h \sum_{i=1}^{N} \left(\frac{1}{Le_i} - 1\right) \frac{\partial Q_i}{\partial \eta}, \end{aligned} \tag{2}$$

where the terms including the i-th species Lewis number Le_i, on the right hand side of each equation, must be considered to capture differential diffusion. Particularly, non-unity Lewis numbers are considered only for H-atom and H_2, i.e., Le_H = 0.18 and Le_{H_2} = 0.3. A star, *, denotes the cross-stream average of the quantity ϕ defined as

$$\phi^* = \frac{\{\phi_\eta P_\eta\}}{\{P_\eta\}} = \frac{\lim_{R\to\infty} \int_{r\leq R} \phi_\eta P_\eta r dr}{\lim_{R\to\infty} \int_{r\leq R} P_\eta r dr}, \tag{3}$$

where the subscript η indicates conditioning on the sample space variable η of the mixture fraction ξ, i.e., $\phi_\eta = \langle \phi | \eta \rangle$. The equations above can be seen as the 1D equivalent of the ISRN approach presented by Gkantonas et al. [10]. Instead of dealing with volume-averaged quantities, this formulation is based on cross-stream averaging and represents a series of Incompletely Stirred Reactors (ISRs) that bears some similarity with a plug flow reactor approximation including micro-mixing effects. A similar approach has also been proposed in Ref. [11] for studying soot emissions. In Eqs. 1-2, P_η is modelled as a clipped-Gaussian PDF, N_η is calculated from either the AMC model [9] or the approach proposed by Devaud et al. [12]. In the latter, N_η is derived directly from the double integration of the PDF transport equation of the conserved scalar mixture fraction ξ,

$$\frac{\partial}{\partial z}(\rho_\eta U^* P^*) = -\frac{\partial^2}{\partial \eta^2}(\rho_\eta N^* P^*), \tag{4}$$

and the double integration is carried out as follows

$$N^* = \frac{1}{\rho_\eta P^*}\frac{\partial}{\partial z}\left[\int_\eta^1 \rho_\eta U^* P^*(\eta')(\eta - \eta') d\eta'\right]. \tag{5}$$

The double integration of the averaged PDF P^*, however, leads to numerical problems when $P^* \to 0$. A "quasi-consistent" approach is here employed to combine N^*_{DI} from double integration to the N^*_{AMC} from AMC. The criterion for the double integration-AMC switch is based on the quantity N^*P^*. At regions where $N^*P^* \to 0$ and $\Delta(N^*P^*) > \epsilon$ (where ϵ is a user-defined threshold), N^* is taken from AMC whereas the doubly integrated value is kept elsewhere. This makes the approach hybrid and "quasi-consistent" since N^* is exact where it matters most. M^* is calculated by cross-stream averaging the conditionally filtered diffusion term M_η, modelled here as

$$M_\eta = \frac{1}{\rho P_\eta}\frac{\partial}{\partial \eta}(\rho P_\eta N_\eta). \tag{6}$$

In Eq. 2, the term $\langle \dot{\zeta}_i | \eta \rangle$ accounts for the convective and radiative heat transfer from the gaseous phase to the quartz tube and is modelled according to Hall [13] for the radiative part and Hergart and Peters [14] for the convective part. The kinetic mechanism for hydrogen of Kéromnès et al. [15] (15 species, 48 reactions) is employed here.

One must notice that the ISRN approach does not account for thermal expansion since it takes an inert flow solution as input. However, for the problem of autoignition, where only small density changes are expected to occur before autoignition happens, post-processing non-reacting flow mixing patterns introduces only small errors.

3 Results

The ISRN equations are solved in post-processing on top of the inert mixing field resolved by LES. The "equal velocity" experimental case, where the inlet mean velocities of fuel and air streams are identical U_f=U_{ox}=26 m/s, is targeted. The validation of the LES mixing field has been performed on the measured mean and rms of axial velocity at z=2 mm above the inlet and on the measured mixture fraction and mixture fraction variance profiles along the centerline. The autoignition length is defined based on the H-radical, at the location of the maximum gradient of the H-radical mass fraction. Little difference with OH*, OH, O or T are observed. First, the effect of the modelling of the conditional scalar dissipation rate is evaluated. The scalar dissipation rate is expected to be influential on autoignition [1]. The autoignition lengths obtained with the conditional scalar dissipation rate N_η from the AMC model and the quasi-consistent (QC) approach at different inlet air temperature T_{ox} are shown in Fig. 2a. The predicted values are compared with both the minimum and mean autoignition lengths (indicated by L_{min} and $\langle L_{ign} \rangle$, respectively) reported by Markides and Mastorakos [2] and related to the appearance of OH chemiluminescence. Unity Lewis number, constant inlet fuel temperature, T_f=855 K, and adiabatic conditions are also considered in the simulations.

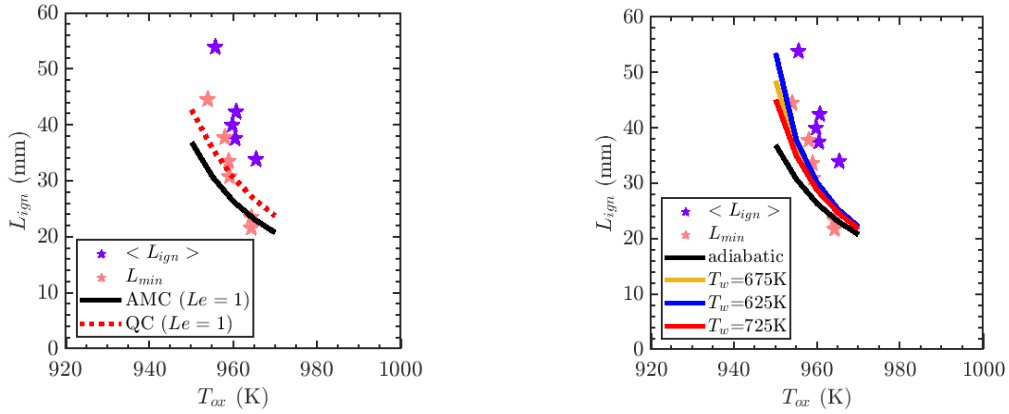

(a) (b)

Figure 2: Autoignition lengths for hydrogen at different inlet air temperatures T_{ox}. Minimum L_{min} and mean $\langle L_{ign} \rangle$ from experiments and L_{ign} predicted by ISRN: (a) with N_η from the AMC model and the quasi-consistent (QC) approach; (b) with N_η from the AMC model, adiabatic conditions, and non-adiabatic conditions with three different wall temperatures T_w= 625,675,725K.

From Fig. 2a, it can be seen that the autoignition length decreases with increasing inlet air temperature, in accordance with experiments and with other numerical studies. The autoignition trend is captured fairly well, and higher autoignition lengths L_{ign} are obtained when the quasi-consistent approach for the scalar dissipation rate is considered.

The autoignition lengths obtained with N_η from the AMC model at different inlet air temperature T_{ox} and non-adiabatic conditions are shown in Fig. 2b. The effect of the wall temperature on autoignition are quantified by considering three different temperatures, i.e. T_w= 625, 675 and 725 K. Unity Lewis number and constant inlet fuel temperature, T_f=855 K are again considered. The curve obtained for the same settings but at adiabatic conditions is also shown for comparison. The autoignition length increases at non-adiabatic conditions with respect to adiabatic conditions at all T_{ox}. A decrease of the wall temperature determines an increase of the autoignition length. The autoignition length is more sensitive to the wall temperature at lower inlet air temperatures T_{ox} <960 K.

The effect of differential diffusion on autoignition is examined next. The autoignition lengths obtained with N_η from the AMC model at different inlet air temperature T_{ox}, U_f=U_{ox}=26 m/s, inlet fuel temperature T_f=855 K, non-adiabatic conditions with T_w=675 K and non-unity Lewis number are shown in Fig. 3a. Although the trend is not significantly affected, the autoignition lengths slightly decrease due to differential diffusion of molecular hydrogen and H-radical. The autoignition length is more sensitive to differential diffusion at lower inlet air temperatures T_{ox} <960 K.

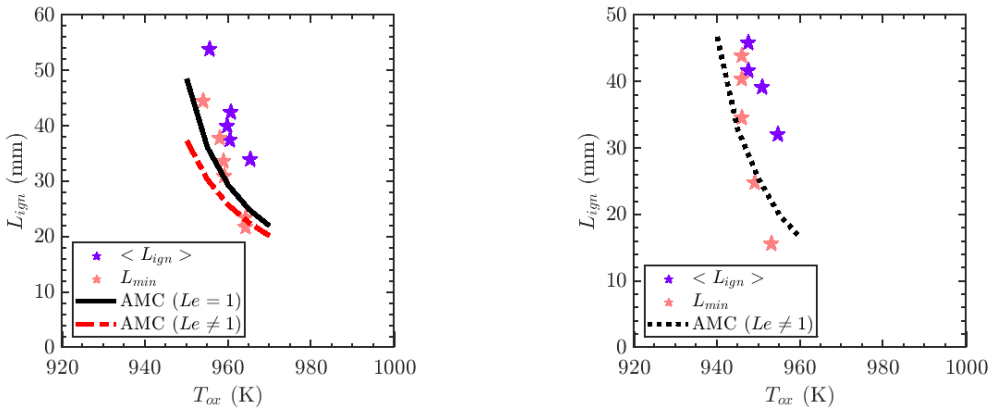

Figure 3: Autoignition lengths for hydrogen at different inlet air temperatures T_{ox} and: (a) U_f=U_{ox}=26 m/s; (b) U_f=U_{ox}=20 m/s. Minimum L_{min} and mean $\langle L_{ign} \rangle$ from experiments and L_{ign} predicted by ISRN with N_η from the AMC model, T_w=675 K, with and without differential diffusion.

A different equal velocity case, i.e. U_f=U_{ox}=20 m/s, is simulated by the ISRN approach with N_η from the AMC model at different inlet air temperatures T_{ox}, inlet fuel temperature T_f=855 K, non-adiabatic conditions with T_w=675 K and differential diffusion. The results of Fig. 3b show good agreement with the experimental values.

4 Preliminary conclusions

In this work, an Imperfectly Stirred Reactor Network (ISRN) approach has been employed to predict the autoignition behaviour of hydrogen in a turbulent co-flow of preheated air. The ISRN equations are solved in post-processing on top of a well-resolved inert flow LES of the continuous, axisymmetric fuel plume into the stream of preheated, turbulent air confined by an outer quartz tube. The effect of non-adiabatic conditions and differential diffusion on the prediction of autoignition lengths has been studied. The results show that the approach is able to well capture the autoignition behaviour of hydrogen, and that the autoignition location is sensitive not only to the inlet air temperature but also to the average wall temperature and the presence of differential diffusion. Moreover, the sensitivity is higher at lower inlet

air temperatures. This study represents the first successful application of a computationally-cheaper CMC-based reacting flow simulation methodology that can be used on top of inert LES simulations to estimate the effect of micromixing on autoignition and the autoignition propensity for a range of combustion device designs and operating conditions.

References

[1] Mastorakos E. (2009). Ignition of turbulent non-premixed flames. Prog. Energy Combust. Sci. 35:57.

[2] Markides CN, Mastorakos E. (2005). An experimental study of hydrogen autoignition in a turbulent co-flow of heated air. Proc. Combust. Inst. 30: 883.

[3] Klimenko AY, Bilger RW. (1999). Conditional moment closure for turbulent combustion. Prog. Energy Combust. Sci. 25:595.

[4] Jones WP, Navarro-Martinez S. (2008). Study of hydrogen auto-ignition in a turbulent air co-flow using a large eddy simulation approach. Comput. Fluids 37: 802.

[5] Patwardhan SS, Lakshmisha KN. (2008). Autoignition of turbulent hydrogen jet in a coflow of heated air. Int. J. Hydrogen Energy 33:7265.

[6] Buckrell AJM, Devaud CB. (2013). Investigation of mixing models and conditional moment closure applied to autoignition of hydrogen jets. Flow Turbul. Combust. 90:621.

[7] Navarro-Martinez S., Kronenburg A. (2011). Flame stabilization mechanisms in lifted flames. Flow Turbul. Combust. 87:377.

[8] Stanković I, Triantafyllidis A, Mastorakos E et al. (2011). Simulation of hydrogen auto-ignition in a turbulent co-flow of heated air with LES and CMC approach. Flow Turbul. Combust. 86:689.

[9] O'Brien E, Jiang TL. (1991). The conditional dissipation rate of an initially binary scalar in homogeneous turbulence. Phys. Fluids 3:3121.

[10] Gkantonas S, Foale JM, Giusti A, Mastorakos E. (2020). Soot emission simulations of a single sector model combustor using incompletely stirred reactor network modeling. J. Eng. Gas Turbines Power 142(10):101007

[11] Gkantonas S. (2021). Predicting soot emissions with advanced turbulent reacting flow modelling. PhD thesis, University of Cambridge.

[12] Devaud CB, Bilger RW, Liu, T. (2004). A new method of modeling the conditional scalar dissipation rate. Phys. Fluids 16(6):2004.

[13] Hall RJ. (1988). Computation of the radiative power loss in a sooting diffusion flame. Appl. Opt. 27(5):809.

[14] Hergart C, Peters N. (2002). Applying the Representative Interactive Flamelet Model to Evaluate the Potential Effect of Wall Heat Transfer on Soot Emissions. J. Eng. Gas Turbines Power 124(4):1042.

[15] Kéromnès A, Metcalfe WK, Heufer KA et al. (2013). An experimental and detailed chemical kinetic modeling study of hydrogen and syngas mixture oxidation at elevated pressures. Combust. Flame 160(6):995.